eor.istanbul.edu.tr

Official Publication of Istanbul University Faculty of Dentistry

Eur Oral Res 2018; 52: 12-8.

Original research

Alkaline phosphatase levels of murine pre-osteoblastic cells on anodized and annealed titanium surfaces

Sinem Yeniyol[1], John Lawrence Ricci[2]

Purpose
This study aimed to evaluate the initial adhesion morphology and alkaline phosphatase (ALP) activity of murine pre-osteoblastic MC3T3-E1 cells cultured on anatase/rutile mixed-phase TiO_2 thin films with photocatalytical activity with previously confirmed antibacterial properties.

Materials and methods
Anatase/rutile mixed-phase TiO_2 thin films fabricated by anodization and annealing of cpTi were used to culture MC3T3-E1 cells to evaluate the initial cellular adhesion morphology and ALP activity in vitro.

Results
Compared with MC3T3-E1 cells cultured on cpTi substrates and the control group, cells cultured on anatase/rutile mixed-phase TiO_2 thin films exhibited similar ALP levels after cell culture day 9.

Conclusion
Anodizing and annealing processes fabricate multifunctional surfaces on cpTi with improved osteogenic properties for implants.

Keywords: *Titanium dioxide, surface roughness, crystal phase, alkaline phosphatase, pre-osteoblastic cell*

Introduction

Titanium and its alloys are widely used for dental implants due to their periimplant bone formation without tissue rejection. After the installation of an implant, implant surface comes in contact with the bone. Bone implant contact is surface dependent and sensitive to surface properties of the implant. The extent of incorporation of the implants is determined by the surface roughness, topography and chemical composition (1). Surface topography and chemistry were reported to influence osteoblast responses and the osseointegration between bone and implant (2). Greater surface roughness increased the total surface area, therefore creating more available surface sites for favorable cellular interactions as cellular adhesion, proliferation, spreading, motility, aggregation and maturation (3-5). Hence, surface modification techniques were deliberated to fabricate microscale to nanoscale structures on Ti surface to simulate the architecture of human bone surface and promote attachment of the osteoblasts (6). Surface chemistry is the other factor which affects the cellular response of the osteoblast cells. The thickness and crystalline structures of titanium dioxide (TiO_2) layers have been associated to influence the bioactive properties of the implant material (7). Since the proposition of photocatalytical oxidation by Fujishima and Honda (8), TiO_2 have gained great attention as a promising photocatalyst. The photocatalytic activity of TiO_2 is most significantly

[1]*Department of Oral Implantology, İstanbul University, Faculty of Dentistry, İstanbul, Turkey*

[2]*Department of Biomaterials and Biomimetics, New York University College of Dentistry, New York, USA*

Corresponding Author: Sinem Yeniyol
E-mail: yeniyols@istanbul.edu.tr

Received: 14 March 2017
Revised: 01 August 2017
Accepted: 28 September 2017

DOI: 10.26650/eor.2018.78387

How to cite: *Yeniyol S, Ricci JL. Alkaline phosphatase levels of murine pre-osteoblastic cells on anodized and annealed titanium surfaces. Eur Oral Res 2018; 52: 12-8.*

influenced by crystalline structure (9). TiO_2 is usually used as a photocatalyst in two crystal structures: rutile and anatase. Considerable surface treatment and modification techniques were attempted to synthesize anatase/rutile mixed-phase TiO_2 such as sol-gel method (10), sputtering (11), chemical vapour deposition (12), atomic layer deposition (13), plasma immersion ion implantation (14), cathodic arc deposition (15), and anodization (16). Among these methods, anodization is an economic and efficient technique that allows controlled anatase/rutile mixed phase TiO_2 formation on the substrates that have been widely employed to biologically modify Ti implants.

Alkaline phosphatase (ALP) is a membrane-bound glycoprotein well known as an early osteogenic marker of bone formation and bone calcification, secreted by osteoblasts to provide a high phosphate concentration at the osteoblast cell surface during bone mineralization (17). Nano-surfaces (refers to the scale from 0.1 nm to 100 nm) could promote the proliferation of osteoblasts and increase the content of alkaline phosphatase after osteoblasts were cultured for 21 to 28 days (18). Non-selective actions of the highly oxidized species are expected to oxidize the cell membrane on the surface of the illuminated TiO_2 (19). However, dental implants are in contact with osteoblasts when they are placed into the bone and these modified surfaces need to be evaluated in terms of osteoblastic adhesion and ALP activity. In this way, a thorough understanding of the photocatalytical cell killing mechanisms at the periimplant osteogenic cells should be questioned in conjunction with their suggested killing effect on oral bacteria.

We suggested that anatase/rutile mixed-phase TiO_2 thin films, prepared by electrochemical anodization with potassium hydroxide and annealing treatment, would have significant effects on the initial adhesion morphology and ALP activity of murine pre-osteoblastic cells *in vitro*. To address this hypothesis, the aim of this study was to assess the cellular response of the murine pre-osteoblastic cells on anatase/rutile mixed-phase TiO_2 thin films which combined the nanoscale roughness characterization and photocatalytical activity by electrochemical anodization.

Materials and methods

Preparation of samples

This study was performed at the laboratories of New York University College of Dentistry and was supported by İstanbul University Fund of Scientific Research (BEK-2017-25356). Commercially pure titanium (cpTi) (ASTM B265-02) sheets in squares (10×10×1 mm) were used as substrates for the experiments as described previously by Yeniyol *et al.* (9). The surfaces of the specimens were prepared by standard metallographical techniques. These sheets were ultrasonically cleaned in acetone, distilled water, and methanol, respectively. These untreated cpTi sheets were named as Group Ti. The electrochemical anodization was employed to form TiO_2 thin films on the cpTi sheets. Anodization voltage was performed under 40V and each Ti surface (anode) was electrochemically anodized in 0.1M KOH electrolyte for 3 minutes at 20°C. Stainless steel was used as the counter electrode. In order to convert the amorphous TiO_2 thin films into the crystallized TiO_2 thin films, sheets were annealed at 550°C in air for 1 h after anodization treatment. These sheets containing mixed-phase TiO_2 thin films consisting of anatase and rutile were named as Group AR.

Surface characterization

The surface morphologies of the sheets were observed using a scanning electron microscope (SEM; JSM5410, JEOL, Tokyo, Japan) at a 20 kV acceleration voltage and a magnification of ×500.

The surface topologies of the sheets were investigated with the White Light Optical Profiling (WLOP) Wyko-NT1100 (Veeco Instruments Inc., Plainview, NY, USA) at VSI (Vertical Scanning Interferometer) mode, which is a noncontact optical profiling system that provides high vertical resolution. Two height descriptive parameters of roughness as $R\alpha$ and Rz were used to quantify the surface roughness (9).

The structure and phase of the Group Ti were monitored by utilizing a Philips PW 3710 grazing incidence x-ray diffractometer with a CuKα radiation (scan range 20° to 80°). A scan rate of 0.02°/sec was used with a grazing incidence of 0.5° for the Ti structure. The structure and phase of the Group AR were monitored by utilizing a Panalitical diffractometer (Phillips, Holland) using X-ray diffraction data collected in the reflection Bragg-Brentano geometry with a CuKα radiation under an applied voltage of 45 kV and a current of 40 mA. A scan rate of 0.03°/sec with a grazing incidence of 0.45° was used for the Ti and TiO_2 structure. The scanning data were recorded in the 2θ range of 20–73°. The phase contents of rutile and anatase (%W_A) and rutile (%W_R) for the anatase/rutile mixed-phase TiO_2 thin films at Group AR were estimated by utilizing the obtained patterns to determine weight percentage of the anatase phase and rutile phase TiO_2 using the Spurr–Myers' equations (9).

Cell assay

In order to determine the impact of the electrochemical anodization and annealing on the biological properties of pre-osteoblasts, MC3T3-E1 were cultured on cpTi sheets submitted to the experimental conditions. Pre-osteoblastic MC3T3-E1 cells (ATCC, Rockville, MD, USA) were cultured in α-MEM (Gibco, California, CA, USA), supplemented with 10% fetal bovine serum (Hycolone, Utah, UT, USA), penicillin and streptomycin (Gibco, California, CA, USA) mixture employed as a cell culture medium. The cells were incubated at 37°C in a humidified atmosphere of 5 % CO_2 in air. The culture medium was changed every 2 d. Specimens were sterilized in 70% ethanol. Cells were seeded onto Group Ti sheets and Group AR sheets at a density of 10.000 cells/sheet in black 24-well polystyrene culture plates for non-UV based conditions. Polystyrene culture plate sheets in squares (10×10×1 mm) were used as positive controls (Control Group).

Cell morphology

Sheets were collected for SEM observation after 5 days to study cells' morphological changes during initial adhesion of MC3T3-E1 cells cultured on both experimental and control

surfaces. The samples were fixed with 2.5% glutaraldehyde. After washing three times in the 0.1M phosphate buffer, cells were postfixed with 1% OsO_4 for 1 h. After sheets were rinsed twice in the 0.1M phosphate buffer, they were dehydrated through a graded alcohol series (25–100%). Hexamethyldisilazane was applied twice. Sheets were subsequently critical-point dried; sputter coated with gold, and examined using a scanning electron microscope (SEM; Philips XL 30, Eindhoven, The Netherlands) at a 15 kV accelerating voltage and a x500 magnification.

Alkaline phosphatase activity

The differentiation of pre-osteoblast to osteoblast cells was evaluated as a function of alkaline phosphatase (ALP) activity for 5, 9, 12 and 21 days by ELISA method. Samples of various groups were transferred into a new black 24-well polystyrene culture plate and the cell layers were washed with PBS. Triton X-100 were added to each well to study lysis of the cells. The material was placed in an incubator for 30 min at 37°C. After 3 times freezing-thawing cycles, aliquots of cell lysis solution were collected for the analysis of the ALP activity. ALP activity was determined with conversion of p-nitrophenylphosphate to nitrophenol in an alkaline buffer. Reaction was initiated by adding of p-nitrophenylphosphate to the cell lysis solution. The reaction was stopped after 20 min by adding NaOH. Optical density (SpectraMax M5e Multi-Mode Microplate Reader; Molecular Devices, Sunnyvale, CA, USA) was measured at 405 nm to quantify the amount of p-nitrophenol produced.

Statistical analysis

All statistical analyses were performed using SPSS 22.0 (IBM SPSS Inc., Armonk, NY, USA). Data were expressed as the mean±standard deviation (n=12). Analysis of the baseline clinical data of ALP activity was performed by Chi-square statistics. We used the Kruskal – Wallis test for comparison of more than two independent groups, followed by the Mann –Whitney U test for comparisons between different groups, and the Friedman's test followed by the Wilcoxon Signed Ranks test for intra-individual comparisons. Differences were considered significant at $p<0.05$ (two tailed value).

Results

Surface characterization

Figure 1 shows surface SEM images of sheets of cpTi (Group Ti) and the mixed-phase TiO_2 thin film photocatalyst (Group AR). It is observed that cpTi surface has a flat texture and showed relatively a smooth appearance. The surface morphology of the photocatalyst was affected by the electrochemical anodization. Craters (2-5 μm) and protruding hills (10-50 μm) were observed in Group AR anodized in the KOH electrolyte, conferring a more pronounced increase of surface roughness compared to cpTi sheets in Group Ti (9).

Quantitative roughness parameters Ra and Rz obtained from WLOP analysis for 1x1.2 mm^2 areas for the Groups Ti and AR are shown in Table 1. Three dimensional images of the surface topography of the Groups Ti and AR at x5.1 magnification are shown in Figure 2. Ra and Rz surface roughness parameters values obtained from the Group AR quantitatively presented higher height descriptive parameters of roughness (9).

The phase compositions of the obtained samples were characterized by XRD and the corresponding XRD patterns are shown in Figure 3. There were no anatase or rutile diffraction peaks observed in cpTi surfaces in Group Ti. After anodization treatment and annealing at 550°C for 1 h, the mixed-phase composition of the Group AR was confirmed by its XRD patterns in Figure 3, where two sharp peaks located at the 2θ values of 38.4° and 27.4°, which are attributed to the diffraction of the (004) crystal plane of anatase TiO_2 and the (110) crystal plane of rutile phase TiO_2, respectively, indicating the crystallinity of the structure. Other characteristic peaks of the different crystalline phases are also marked on the pattern (Ti: Titanium; A: Anatase; R: Rutile). Anatase and rutile contents (weight percentages) in each sample were confirmed by using Spurr–Myers' equations and the corresponding results of anatase and rutile were calculated as 54.6 wt% and 41.9 wt%, respectively (9).

Cell assay

Cell morphology was examined by using SEM analysis. It was found that cells were able to adhere to the Group Ti sheets and Control Group with similar cellular morphologies indicating healthy behavior and significantly longer configuration at day 5 (Figures 4b, c). Well-defined cytoplasmic cell extensions, namely filopodia and lamellipodia, of these flat cells were attached to the surface increasing the cell–material interaction as well as showing extracellular interaction with the neighboring cells.

In contrast to these findings, there were morphological change in cell morphology on the surface of the Group AR sheets (Figure 4a). SEM analysis showed that the electrochemically anodized and annealed surfaces exhibited bursted cell morphology. Cells were found separated from each other with no communication and no existence of filopodia or lamellipodia. The extracellular matrix in Group AR were improved and the network were found strong enough to cover the whole surface. In this present case, extracellular matrix was influenced by surface chemistry or the surface roughness.

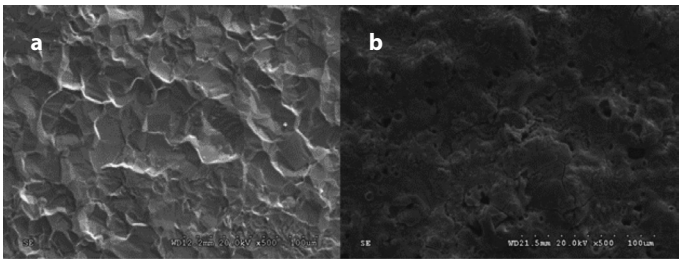

Figure 1. a, b. *Representative top-view SEM micrographs of the (a) Group Ti, and (b) Group AR. (original magnification x500; bar=100 μm). SEM: scanning electron microscope; AR: AnataseRutile; Ti: Titanium; cpTi: commercially pure titanium.*

Alkaline phosphatase activity

Figure 5 shows the ALP activity of murine pre-osteoblastic MC3T3-E1 cells on the different surfaces over the cell culture period. The ALP activity of the cells on Group AR was lower than that on Group Ti after 5 days (p=0.002). However, Group AR reached its highest ALP value at day 12, no significant differences were found between the three groups for the days 9, 12, and 21 (p=0.0694, p=0.742, and p=0.849, respectively).

Within the groups for time intervals, ALP levels of Group Ti significantly decreased at day 21 compared to the days 5, 9, and 12 (p=0.006, p=0.019, and p=0.041, respectively). ALP levels of Control Group significantly decreased at day 21 compared to the days 9 and 12 (p=0.034 and p=0.041, respectively) and ALP levels of Group AR significantly decreased at day 12 compared to the day 5 (p=0.015) revealing that ALP activity was surface roughness and crystalline structure dependent.

Table 1. *Ra (arithmetical mean roughness) and Rz (ten-point mean roughness) of the Groups Ti and AR determined by WLOP for 736X480 µm² areas. Data are presented as the mean±SD (Standard Deviation). Values are in micrometers (µm) (9)*

Groups	R_a (µm)±SD	R_z (µm)±SD
Ti	1.51±0.02	12.76±0.04
AR	4.08±0.02	42.40±0.27

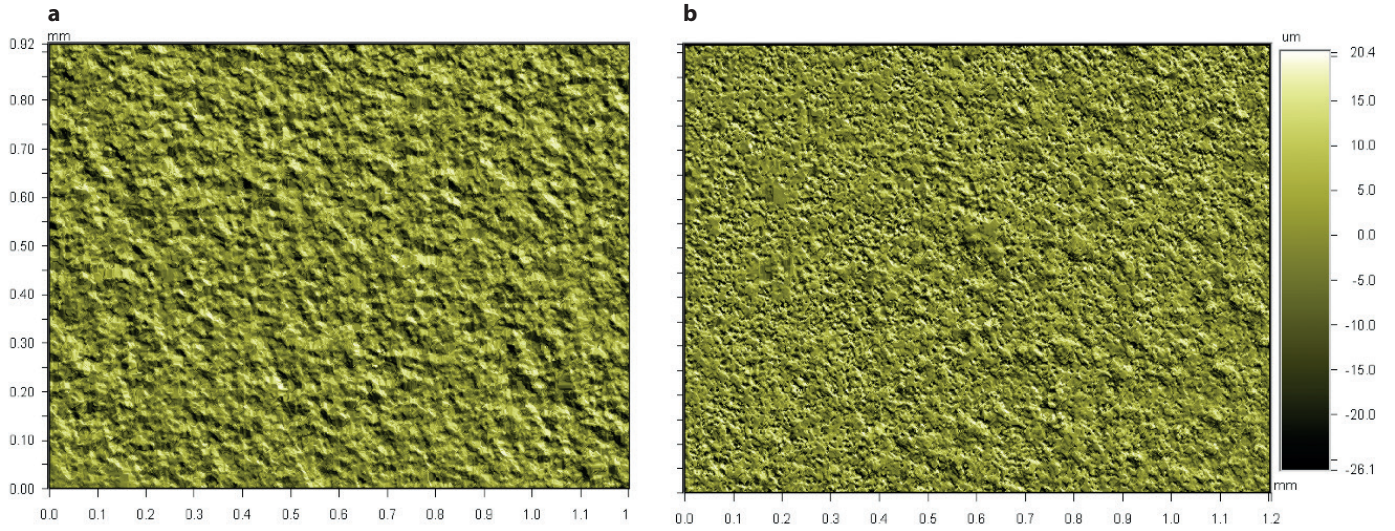

Figure 2. a, b. *Representative WLOP images of (a) Group Ti, and (b) Group AR at x5.1 magnification for 1 x 1.2 mm² of area (9).*

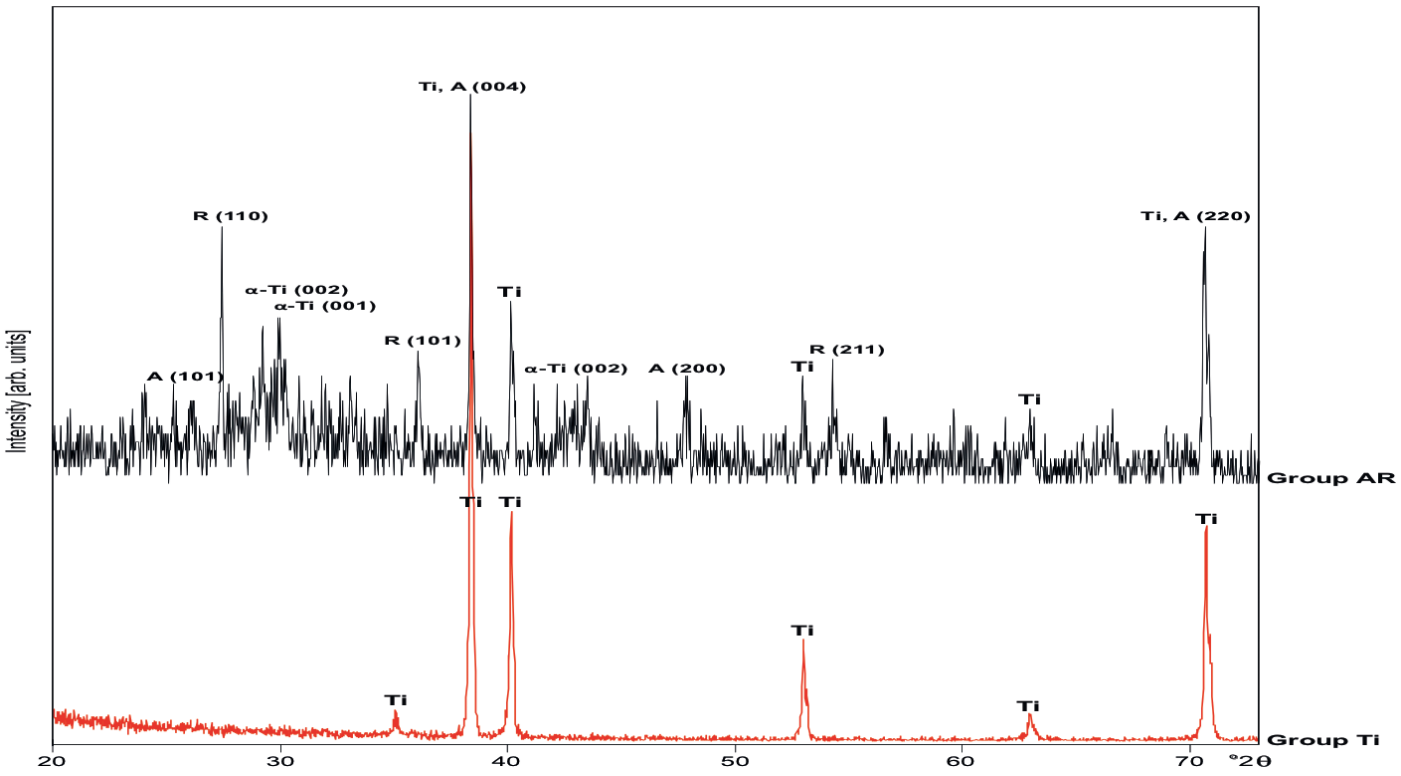

Figure 3. *X-ray diffraction patterns of Group Ti: cpTi surface; Group AR: anatase/rutile mixed-phase TiO_2 thin film surface (Ti: titanium; A: anatase; R: rutile) (9).*

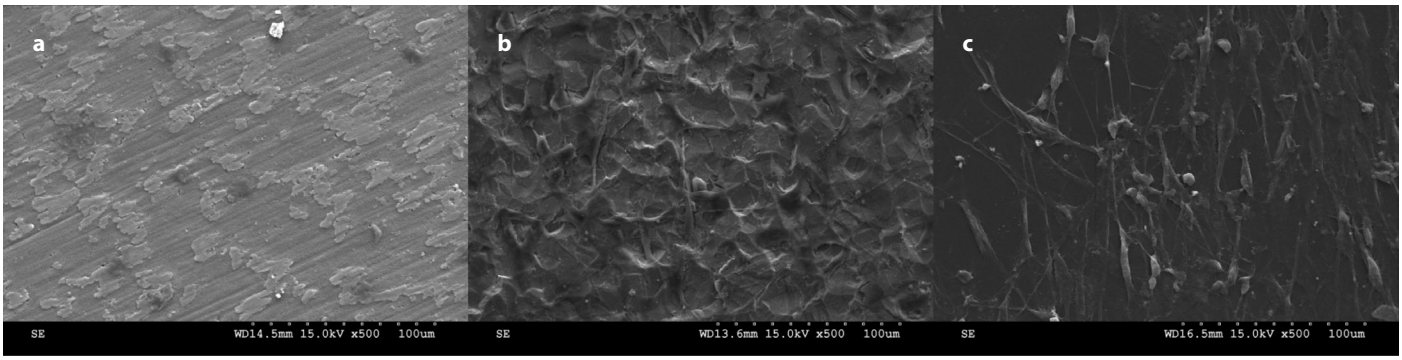

Figure 4. a-c. *Representative SEM micrographs illustrating cell adhesion morphology on; (a) Group AR; (b) Group Ti; and (c) Control group (tissue culture polystyrene) (original magnification x500; bar=100 µm).*

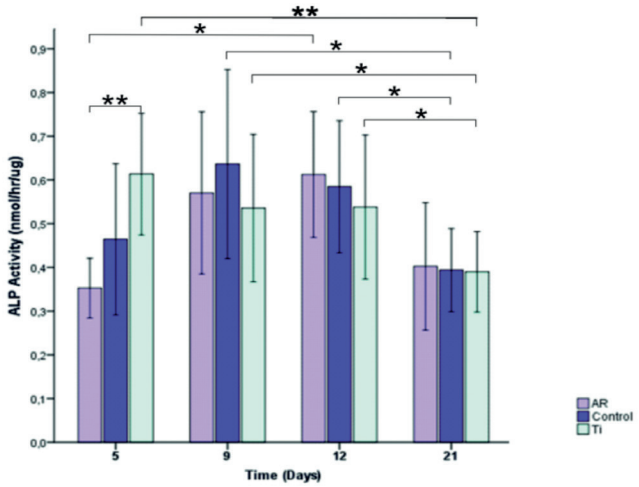

Figure 5. *Histogram showing ALP activity of MC3T3-E1 pre-osteoblast cells at 5, 9, 12, and 21 days. Data are Means±SDs of absorbance values of the experimental and control groups (*p<0.05, and **p<0.01).*

Discussion

The aim of this study was to evaluate *in vitro* pre-osteoblastic initial cell adhesion morphology and ALP activity at the anatase/rutile mixed-phase TiO_2 thin film coated surfaces, prepared by electrochemical anodization with potassium hydroxide and annealing treatment.

Based on our previous study (9), by aiming to gain a better understanding of the surface roughness and crystalline structure of anatase and rutile, more active surface sites for reactions by higher photocatalytic reaction potential were created to be utilized for transmucosal components of dental implants to interpret the antibacterial clinical performance of these parts in relation to the intra oral usage sites. Anatase/rutile mixed-phase TiO_2 thin films were found to inhibit the adhesion of A. actinomycetemcomitans under UV light irradiation confirming enhanced photoactivity. This objective was achieved via electrochemical anodization by KOH and annealing of the cpTi substrates. This surface modification of the cpTi in Group AR specimens in the nano-scale regime, created craters (2–5µm) and protruding hills (10–50µm) conferring a more pronounced increase of surface roughness compared to cpTi specimens in GroupTi (Figure 1). Quantitative roughness parameters $R\alpha$ and Rz, obtained from WLOP analysis, quantitatively presented higher height descriptive parameters of roughness for the anatase/rutile mixed-phase TiO_2 thin films in Group AR (Figure 2, Table 1) (9). SEM observations showed that the pre-osteoblast cells were well spread and attached onto both Group Ti and Control Group surfaces at day 5. In Figures 4b and 4c, the cells were oriented with filopodia and lamellipodia. In contrast to these findings, on the surface of the Group AR, bursted cell morphology as well as improved extracellular matrix formation were evident (Figure 4a). In consequence, surface topography was effective on the cellular response in the early phase of cellular proliferation.

Nanostructured alkali-metal titanates are utilized in applications including catalysis, photocatalysis, bioelectrocatalysis, hydrogen storage, lithium batteries, and solar cells (20). Sodium hydroxide and/or heat treatment, hydrogen peroxide treatment of Ti substrates have been widely used to enhance the biocompatibility and corrosion resistance of the implants in addition to their photocatalytic activities (21-24). When subjected to NaOH and KOH alkali and followed by heat treatment; formation of respective titanates as sodium titanate and potassium titanate on cpTi had been found superior owing to their mechanical properties and corrosion resistances. These bioactive surfaces were found to form a bone-like apatite layer on their surfaces when immersed in simulated body fluid providing earlier fixation of the implants (25). Tas and Bhaduri (26) were the first to soak Ti sheets in a 5 M KOH solution at 60°C for 24 h and 600°C heating for 1 h in air, followed by coating these alkali-modified surfaces with an apatitic calcium phosphate layer by using a supersaturated SBF. The microporous layer formed in the 5 M KOH solution were found to develop faster and thicker under anodization with superior to the analogous layer prepared in the 5 M NaOH solution by Tanaka *et al.* (27). Cai *et al.* (21) applied alkali treatment with immersion of cpTi discs into KOH solutions at concentrations of 4, 6, 8, and 10 M at 600°C for 24h followed by heat treatment at 600°C for 1h. This KOH alkali immersion treatment presented peaks attributed to anatase Ti and $K_2Ti_4O_9$ confirming anatase and potassium titanate formation on titanium substrate surfaces. KOH alkali treatment and heat treatment was found to increase corrosion resistance and induce the differentiation of murine mesenchymal stem cells into osteoblasts. In our study, anodic oxidation with 0.1 M KOH solution and annealing treatment were applied instead of immersion technique. In Group AR, corresponding results of anatase and rutile were calculated as 54.6wt% and 41.9wt%, respectively whereas Group Ti presented no anatase or rutile peaks, as previously described (Figure 3) (9). The chemical composition of the surfaces attribute to this result. Atomic structure of the substrate confined by its crystallographic orientations and its

interaction with the cell at nanoscale level must be controlled for the interface modeling between bone and the implant surface. Similar chemical compositions with different crystallographic textures can affect the biological responses of the cells (28).

Most works applying anodic oxidation and annealing on the preparation of titanium oxide thin films have reported on the formation of titanium oxide nanotubes, nanofibers, and nanowires (29-31). The effect of heat treatment on these structures was studied to form anatase titania having higher specific surface area compared to rutile which is important for the enhancement of photocatalytic property of the oxide (32).

The formation of self-organized TiO_2 nanotubes in fluoride containing electrolytes via electrochemical anodization is an attractive way with the ability to couple with other surface treatments such as thermal oxidation, coatings, nanotube doping, and drug-loading (1). The presence of nanophase surfaces and amorphous TiO_2 on Ti and Ti-alloys have been shown to render available sites for protein adsorption and cell–implant interaction (33). In our study, electrochemically anodized and annealed cpTi surfaces presented non-tubular TiO_2 thin film coated nanophase surfaces (Figure 1).

Alkaline phosphotase activity is used as an initial marker of cellular differentiation (34). These two groups of cpTi substrates having different surface roughness and crystallographic textures were used to assess the effects of surface roughness and crystal orientation on pre-osteoblast cell differentiation by measuring ALP activity in addition to its previous proven photocatalytical activity (9). In our experiment the ALP activity significantly decreased for that anatase/rutile mixed-phase TiO_2 thin films at Group AR at day 5 compared to the cpTi surfaces at Group Ti, whereas this difference became insignificant after the days 9, 12 and 21, which indicated that the osteogenetic activity of these cells was stable during this time (Figure 5).

The results of this present study show that anatase/rutile mixed-phase TiO_2 thin films fabricated by electrochemical anodization in KOH and annealing, which is responsible for the antibacterial properties, *per se* does not increase but it does not limit either pre-osteoblastic initial cell adhesion morphology and ALP activity at non-UV conditions *in vitro*. Anatase/rutile mixed-phase TiO_2 thin films fabricated by electrochemical anodization and annealing can be a promising option considered for the short-term antibacterial improvement applications for the implants.

Conclusion

Anatase/rutile mixed-phase TiO_2 thin films fabricated by electrochemical anodization in KOH and annealing showed slightly better differential response of pre-osteoblastic cells than cpTi during 21-days cell culture period, offering a choice to be a candidate for the surface of implant materials. However, for better understanding of photocatalytical mechanisms involved in the application of this material under UV-based conditions focused on cell-substrate interactions, experimental conditions should be tested under UV-based conditions to better understand the whole destructive effect of this surface over cellular behaviors in further *in vitro* studies. It is difficult to simulate the real *in vivo* conditions, using murine pre-osteoblasts, as this study was carried out under laboratory conditions. Therefore, further in *vitro* and *in vivo* studies are warranted to demonstrate the influence of such anodization treatments on the cellular response of osteoblast cells. The findings, however, have to be verified in clinical settings.

Ethics Committee Approval: Not required.

Informed Consent: Not required.

Peer-review: Externally peer-reviewed.

Author Contributions: SY designed the study, generated, gathered and analyzed the data, wrote the majority of the original draft. JLR designed the study and generated the data. All authors approved the final version of paper.

Conflict of Interest: No conflict of interest was declared by the authors.

Financial Disclosure: This study was performed at the laboratories of New York University College of Dentistry and was supported by Istanbul University Fund of Scientific Research (BEK-2017-25356).

Türkçe öz: *Anodizasyon ve ısıl işleme maruz bırakılmış yüzeylere karşı pre-osteoblastik fare hücrelerinin alkalen fosfataz seviyeleri. Amaç: Bu çalışmanın amacı; daha önce antibakteriyel özelliği teyit edilen ve fotokatalitik olarak aktif olan anatas/rutil karışımı fazındaki TiO_2 ince film kaplamalara yönelik pre-osteoblastik fare MC3T3-E1 hücrelerinin başlangıç adezyon morfolojileri ile alkalen fosfotaz seviyelerini (ALP) değerlendirmektir. Gereç ve Yöntem: Saf titanyumun anodizasyonu ve ısıl işleme maruz bırakılması ile elde edilen anatas/rutil karışımı fazındaki TiO_2 ince film kaplamalar MC3T3-E1hücreleri ile kültüre edilerek hücrelerin başlangıç adezyon morfolojileri ve ALP aktiviteleri in vitro olarak değerlendirilmiştir. Bulgular: Anodize edilmiş ve ısıl işlem uygulanmış titanyum numuneler üzerinde kültüre edilen MC3T3-E1 hücreleri saf titanyum yüzeyler ve kontrol grubu ile karşılaştırıldığında hücre kültürünün 9. gününden sonra benzer ALP seviyeleri göstermektedir. Sonuç: Anodizasyon ve ısıl işlem uygulamaları ile saf titanyum yüzeyler üzerinde implantlar için osteojenik özelliklerin geliştirildiği multifonksiyonel yüzeyler üretilebilmektedir. Anahtar kelimeler: Titanyum oksit, yüzey pürüzlülüğü, kristal fazı, alkalen fosfataz, pre-osteoblastik hücre*

References

1. Grotberg J, Hamlekhan A, Butt A, Patel S, Royhman D, Shokuhfar T, Sukotjo C, Takoudis C, Mathew MT. Thermally oxidized titania nanotubes enhance the corrosion resistance of Ti6Al4V. Mater Sci Eng C Mater Biol Appl 2016; 59: 677-89. [CrossRef]
2. Wennerberg A, Albrektsson T. Effects of titanium surface topography on bone integration: A systematic review. Clin Oral Implants Res 2009; 20: 172-84. [CrossRef]
3. Anselme K, Bigerelle M, Noel B, Iost A, Hardouin P. Effect of grooved titanium substratum on human osteoblastic cell growth. J Biomed Mater Res 2002; 60: 529-40. [CrossRef]
4. Cooper LF, Masuda T, Yliheikkila PK, Felton DA. Generalizations regarding the process and phenomenon of osseointegration. Part II. In vitro studies. Int J Oral Maxillofac Implants 1998; 13: 163-74.
5. Nishimoto SK, Nishimoto M, Park SW, Lee KM, Kim HS, Koh JT, Ong JL, Liu Y, Yang Y. The effect of titanium surface roughening on protein absorption, cell attachment, and cell spreading. Int J Oral Maxillofac Implants 2008; 23: 675-80.

6. Stevens MM, George JH. Exploring and engineering the cell surface interface. Science 2005; 310: 1135-8. [CrossRef]
7. Lin YH, Peng PW, Ou KL. The effect of titanium with electrochemical anodization on the response of the adherent osteoblast-like cell. Implant Dent 2012; 21: 344-9. [CrossRef]
8. Fujishima A, Honda K. Electrochemical photolysis of water at a semiconductor electrode. Nature 1972; 238: 37-8. [CrossRef]
9. Yeniyol S, Mutlu I, He Z, Yuksel B, Boylan RJ, Urgen M, Karabuda ZC, Basegmez C, Ricci JL. Photocatalytical antibacterial activity of mixed-phase TiO2 nanocomposite thin films against aggregatibacter actinomycetemcomitans. Biomed Res Int 2015; 2015: 705871. [CrossRef]
10. Yu J, Zhao X, Zhao Q. Photocatalytic activity of nanometer tio2 thin films prepared by the sol–gel method. Mater Chem Phys 2001; 69: 25-9. [CrossRef]
11. Shieh KJ, Li M, Lee YH, Sheu SD, Liu YT, Wang YC. Antibacterial performance of photocatalyst thin film fabricated by defection effect in visible light. Nanomedicine 2006; 2: 121-6. [CrossRef]
12. Byun D, Jin Y, Kim B, Kee Lee J, Park D. Photocatalytic TiO2 deposition by chemical vapor deposition. J Hazard Mater 2000; 73: 199-206. [CrossRef]
13. Kemell M, Pore V, Ritala M, Leskela M, Linden M. Atomic layer deposition in nanometer-level replication of cellulosic substances and preparation of photocatalytic tio2/cellulose composites. J Am Chem Soc 2005; 127: 14178-9. [CrossRef]
14. Mandl S, Sader R, Thorwarth G, Krause D, Zeilhofer HF, Horch HH, Rauschenbach B. Investigation on plasma immersion ion implantation treated medical implants. Biomol Eng 2002; 19: 129-32. [CrossRef]
15. Kepenek B, Öncel S, Çakır AF, Ürgen M. Photoactive tio2 coatings on metal substrates by cathodic arc deposition technique. Euro Ceramics 2004; 264-268: 549-52.
16. Lee K, Kim D, Roy P, Paramasivam I, Birajdar BI, Spiecker E, Schmuki P. Anodic formation of thick anatase TiO2 mesosponge layers for high-efficiency photocatalysis. J Am Chem Soc 2010; 132: 1478-9. [CrossRef]
17. Sharma U, Pal D, Prasad R. Alkaline phosphatase: An overview. Indian J Clin Biochem 2014; 29: 269-78. [CrossRef]
18. Webster TJ, Ergun C, Doremus RH, Siegel RW, Bizios R. Enhanced functions of osteoblasts on nanophase ceramics. Biomaterials 2000; 21: 1803-10. [CrossRef]
19. Blake DM, Maness PC, Huang Z, Wolfrum EJ, Huang J, Jacoby WA. Application of the photocatalytic chemistry of titanium dioxide to disinfection and the killing of cancer cells. Sep Purif Methods 1999; 28: 1-50. [CrossRef]
20. Lee SY, Matsuno R, Ishihara K, Takai M. Electrical transport ability of nanostructured potassium-doped titanium oxide film. APEX 2011; 4: 025803. [CrossRef]
21. Cai K, Lai M, Yang W, Hu R, Xin R, Liu Q, Sung KL. Surface engineering of titanium with potassium hydroxide and its effects on the growth behavior of mesenchymal stem cells. Acta Biomater 2010; 6: 2314-21. [CrossRef]
22. Nishiguchi S, Kato H, Fujita H, Oka M, Kim HM, Kokubo T, Nakamura T. Titanium metals form direct bonding to bone after alkali and heat treatments. Biomaterials 2001; 22: 2525-33. [CrossRef]
23. Ohtsuki C, Iida H, Hayakawa S, Osaka A. Bioactivity of titanium treated with hydrogen peroxide solutions containing metal chlorides. J Biomed Mater Res 1997; 35: 39-47.
24. Wei M, Kimb HM, Kokubo T, Evans JH. Optimising the bioactivity of alkaline-treated titanium alloy. Mater Sci Eng C 2002; 20: 125-134. [CrossRef]
25. Liang F ZL, Wang K. Apatite formation on porous titanium by alkali and heat-treatment. Surf Coat Technol 2003; 165: 133-9. [CrossRef]
26. Tas AC, Bhaduri SB. Rapid coating of ti6al4v at room temperature with a calcium phosphate solution similar to 10× simulated body fluid. J Mater Res 2004; 19: 2742-9. [CrossRef]
27. Tanaka S, Tobimatsu H, Maruyama Y, Tanaki T, Jerkiewicz G. Preparation and characterization of microporous layers on titanium. ACS Appl Mater Interfaces 2009; 1: 2312-9. [CrossRef]
28. Faghihi S, Azari F, Li H, Bateni MR, Szpunar JA, Vali H, Tabrizian M. The significance of crystallographic texture of titanium alloy substrates on pre-osteoblast responses. Biomaterials 2006; 27: 3532-9. [CrossRef]
29. Gong D, Grimes CA, Varghese OK, Hu W, Singh RS, Chen Z, Dickey EC. Titanium oxide nanotube arrays prepared by anodic oxidation. J Mater Res 2001; 16: 3331-4. [CrossRef]
30. Oh S, Daraio C, Chen LH, Pisanic TR, Finones RR, Jin S. Significantly accelerated osteoblast cell growth on aligned TiO2 nanotubes. J Biomed Mater Res A 2006; 78: 97-103. [CrossRef]
31. Yu WQ, Jiang XQ, Zhang FQ, Xu L. The effect of anatase tio2 nanotube layers on MC3T3-E1 preosteoblast adhesion, proliferation, and differentiation. J Biomed Mater Res A 2010; 94: 1012-22. [CrossRef]
32. Lockman Z, Ismail S, Sreekantan S, Schmidt-Mende L, Macmanus-Driscoll JL. The rapid growth of 3 microm long titania nanotubes by anodization of titanium in a neutral electrochemical bath. Nanotechnology 2010; 21: 055601. [CrossRef]
33. Mohan L, Anandan C, Rajendran N. Electrochemical behavior and effect of heat treatment on morphology, crystalline structure of self-organized tio2 nanotube arrays on ti-6al-7nb for biomedical applications. Mater Sci Eng C Mater Biol Appl 2015; 50: 394-401. [CrossRef]
34. Ko HC, Han JS, Bachle M, Jang JH, Shin SW, Kim DJ. Initial osteoblast-like cell response to pure titanium and zirconia/alumina ceramics. Dent Mater 2007; 23: 1349-55. [CrossRef]